Available online at www.sciencedirect.com
SCIENCE DIRECT
Polymer 45 (2004) 5207–5214
polymer
www.elsevier.com/locate/polymer

Preparation and properties of polyamide-6-boehmite nanocomposites

Ceren Özdilek[a], Krzysztof Kazimierczak[b], David van der Beek[c], Stephen J. Picken[a,*]

[a]*Department of Polymer Materials and Engineering, Delft University of Technology, Julianalaan 136, 2826 BL Delft, The Netherlands*
[b]*University of Technology in Wroclaw, 50-373 Wroclaw, Poland*
[c]*Utrecht University, Van't Hoff Laboratory for Physical and Colloid Chemistry, Padualaan 8, 3584 CH Utrecht, The Netherlands*

Received 24 November 2003; received in revised form 11 May 2004; accepted 13 May 2004

Available online 5 June 2004

Abstract

Colloidal boehmite particles have been included into a polyamide-6 matrix by in situ polymerization. The particles have been used without any surface modification. Characterization of the nanocomposites has been carried out using transmission electron microscopy (TEM), dynamical mechanical analysis (DMA) and differential scanning calorimetry (DSC). TEM images indicate that the particles have been homogeneously dispersed in the polymer. DSC results show that the presence of boehmite affects the form of crystallization of polyamide-6, in which case formation of γ-structure is favored over the α-structure and an additional α′-phase is formed. Some mechanical reinforcement of the matrix has been accomplished as indicated by DMA results. The modulus level off at high boehmite concentrations can be explained by the reduction of the crystallinity, which cancels the effect of the filler.

Keywords: Boehmite; Polyamide-6; Nanocomposite

1. Introduction

In recent years, many polymeric composites have been prepared using colloidal particles. The main motivation is to benefit from certain advantages of these particles like electrical/magnetic properties, heat resistance, high modulus and so on. Especially, particles with high anisotropy can account for additional improvement in the mechanical properties of polymers. Most studied polymer-dispersed colloids involve layered systems like clays or plate-shaped systems like kaolin, mica and aluminum hydroxides (Bayerite, Gibbsite)[1]. A few examples about incorporation of boehmite (γ-Al_2O_3) into polymers [2–4] to obtain composite materials are found in literature. In these studies, boehmite is synthesized in several polymer matrices by using the sol–gel method. However, it is not mentioned in any of these studies whether well-defined boehmite particles are formed or not. Here we report the use of well-defined rod-shaped boehmite particles as filler for polymer composites. This system can be an alternative to well-known plate shaped clays and other inorganic fillers.

Boehmite particles are colloidal rod-like species with a high anisotropy. Their aqueous dispersions exhibit flow birefringence, thixotropy and elasticity [5]. Like many of the colloidal rod-like systems, they are capable of forming a nematic phase above a certain particle concentration. In addition to boehmite, well-known inorganic examples that form a nematic phase are imogolite, V_2O_5 and β-FeOOH [6]; whereas cellulose microcrystals, poly(tetrafluoroethylene) whiskers and tobacco mosaic virus are some other examples of organic systems. [5]

In aqueous boehmite dispersions, the particles are stabilized by electrical double-layer repulsion [7]. Addition of an organic solvent destroys the repulsive interaction and results in flocculation of the particles. In order to use the conventional composite preparation techniques (melt-blending/extrusion, solution-blending or in situ polymerization), it is essential to apply surface modification to the particles. So far, in literature, only a few modification methods for boehmite have been reported. In one of these studies, boehmite rods have been coated by silica and then, have further been grafted with *n*-octadecyl alcohol, 3-(methacryloxypropyl) trimethoxy silane [8] or modified polyisobutylene [9], each of which provided a good dispersion of the particles in organic solvents. The other method involved direct grafting of modified polyisobutene

* Corresponding author. Tel.: +31-15-2786946; fax: +31-15-2787415.
E-mail address: s.j.picken@tnw.tudelft.nl (S.J. Picken).

0032-3861/$ - see front matter © 2004 Published by Elsevier Ltd.
doi:10.1016/j.polymer.2004.05.029

on the boehmite surface, providing stabilization of the particles in toluene and cyclohexane [10].

So far, our attempts for modification of boehmite by using several types of silane-based coupling agents have failed, simply because the agents with long alkyl tails are insoluble in water and those that are water-soluble do not provide sufficient organic modification. As the polymer matrix, PA6 was selected because of two facts: first, PA6 is known for its good compatibility with inorganic fillers and clay minerals. And second, its monomer, ε-caprolactam is miscible with water and can polymerize even in the presence of significant amount of water. Thus, it was possible to mix the monomer directly with the aqueous boehmite dispersion. This method avoided the need to modify boehmite rods and to transfer them into organic solvents.

In this study, the main motivation is to include boehmite rods in a polymer in order to obtain mechanical reinforcement, especially in the alignment direction of rods. It is expected that tensile modulus values of the polymer will increase upon boehmite addition. Besides, the formation of a nematic liquid crystalline order may give rise to interesting anisotropic mechanical and optical properties, which may result in novel application areas in the future.

2. Experimental

2.1. Boehmite rods

Colloidal boehmite rods were synthesized according to the method of Buining et al. [11]. The synthesis of particles and their characterization by TEM were done in collaboration with David van der Beek, in the group of H.N.W. Lekkerkerker (Colloid Chemistry Group, Utrecht University).

Boehmite was synthesized by using aluminium isopropoxide (Janssen) and aluminium tri-sec butoxide (Fluka). The aluminium precursors were dissolved in demineralized water that was acidified with 37% hydrochloric acid. The resulting solution was stirred for 1-week to obtain complete hydrolysis of alkoxides, from which polymeric aluminium hydroxides were formed. The latter species were hydrothermally crystallized into boehmite upon autoclaving at 150 °C for 22 h. In order to remove alcoholic by-products, the colloidal dispersions were dialyzed against demineralised water for 1-week. At the end of the synthesis, well-defined boehmite rods dispersed in aqueous medium were obtained. TEM characterization revealed average particle dimensions as 280 nm in length and 20 nm in width. In general, boehmite rods exhibit a high extent of polydispersity. A similar work performed with the same synthesis method using identical amounts of aluminium precursors reports the extent of polydispersity in boehmite rods as 30% in length and width [12].

The final dispersions in water were very stable and no aggregation with time was observed. After dialysis, pH was determined to be 5.5. These dispersions exhibited flow birefringence starting from 0.8% w/w particle concentration; and turned permanently birefringent above 1% w/w; which is the onset of nematic phase formation by these particles with the given dimensions. Usually, in the polymerisations, a boehmite concentration of 1% (w/w) in water was used.

2.2. PA6

For polymerization of ε-caprolactam, the hydrolytic route was chosen [13]. Although anionic polymerization would be less time-consuming, it appears to be less suitable due to the positive charge of the boehmite surface. In the hydrolytic route, water initiates the reaction via opening the caprolactam ring and generating the aminocapronic acid. The polymer then grows by reaction of generated amino acid with the cyclic monomer.

Polymerization reactions were performed in a 500 ml glass reactor equipped with an automatic stirrer and a temperature controller. ε-caprolactam obtained from Fluka was used without further purification. 40 g ε-caprolactam, 10 g aminocaproic acid, 0.25 g adipic acid and 10 ml water were mixed. The mixture was heated at 140–150 °C for 2 h to remove excess water, followed by heating at 230 °C for 4 h. The polymeric product could be poured out while still in the melt. Removal of unreacted monomer and cyclic/ linear oligomers was carried out by Soxhlet extraction (for 12 h) using methanol.

2.3. PA6-Boehmite composites

Synthesis of the composites was carried out according to the method described for PA6. The only difference was the use of aqueous boehmite dispersions instead of water. In Table 1, final boehmite concentrations in PA6 that are obtained by varying the amount of boehmite dispersion used in the polymerization, are reported. These amounts, at the same time, reflect the total water content initially present in the polymerization.

From this point on, the PA6-boehmite samples will be denoted by the codes given in Table 1.

2.4. Sample preparation

Polymerized samples were subjected to extraction and afterwards, they were pressed into thin films by applying an

Table 1
Boehmite contents of the composites determined by TGA and corresponding amounts of aqueous boehmite dispersions used in the polymerization

Sample code	Boehmite content (w/w) (%)	Boehmite dispersion used (ml)
PA6-BL	0	0
PA6-BOE1	1	40
PA6-BOE1.3	1.3	50
PA6-BOE5	5	210
PA6-BOE7.5	7.5	320
PA6-BOE9	9	400

approximate of 180 kN force in a hydraulic press at 250 °C. The final thickness of films was about 0.3 mm. The films were extensively dried for several weeks in a vacuum oven at 80 °C before the characterization steps were carried out.

2.5. Transmission electron microscopy (TEM)

Transmission electron microscopy (TEM) was performed using a Philips CM30T electron microscope with a LaB6 filament operated at 300 kV. Ultramicrotomed slices of our samples were placed on Quantifoil carbon polymer supported on a copper grid. Two of the most concentrated samples, namely PA6-BOE7.5 and PA6-BOE9 were studied by this technique, as it was found from optical polarization microscopy (OPM) that boehmite rods start to orient around these concentrations.

2.6. Differential scanning calorimetry (DSC)

The measurements were performed on a Perkin–Elmer DSC7 differential scanning calorimeter. Samples were heated from 25 to 250 °C at a rate of 10 °C/min and were held for 1 min at the maximum temperature. They were cooled back to 25 °C at a rate of 10 °C/min, which was followed by a second heating run identical to the first heating run.

2.7. Dynamic mechanical analysis (DMA)

Storage moduli of the samples were measured in the extension mode at a frequency of 1 Hz by using a Perkin–Elmer DMA 7e dynamical mechanical analyzer. The measurements were taken in the interval 25–160 °C at a heating/cooling rate of 5 °C/min. Each one of the pressed samples was cut into a small rectangle of 9–7 mm long and 2.5 mm wide. As mentioned above, the thickness was 0.3 mm after the pressing.

2.8. Thermogravimetric analysis (TGA)

The exact amount of boehmite in composite samples was determined by using TGA. The samples were heated from 25 to 800 °C at a rate of 50 °C/min and were kept at this temperature for 30 min. Since PA6 degraded completely without leaving any residue, the remaining part gave us the w/w conc. of our filler. The amount of weight loss as observed by TGA on the pure boehmite (in the form of freeze-dried powder) was taken into account in this measurement.

3. Results and discussion

3.1. Dispersibility of boehmite in PA6s

In Fig. 1(a) and (b), TEM images of the PA6-boehmite composites with two different particle concentrations are shown: 7.5% and 9% w/w. It is clear that boehmite rods are homogeneously dispersed within the polymer matrix. At 7.5% filler concentration, the overall picture shows randomly oriented rods whereas at 9% w/w, it clearly shows parallel nematic orientation of the rods. The arrow in

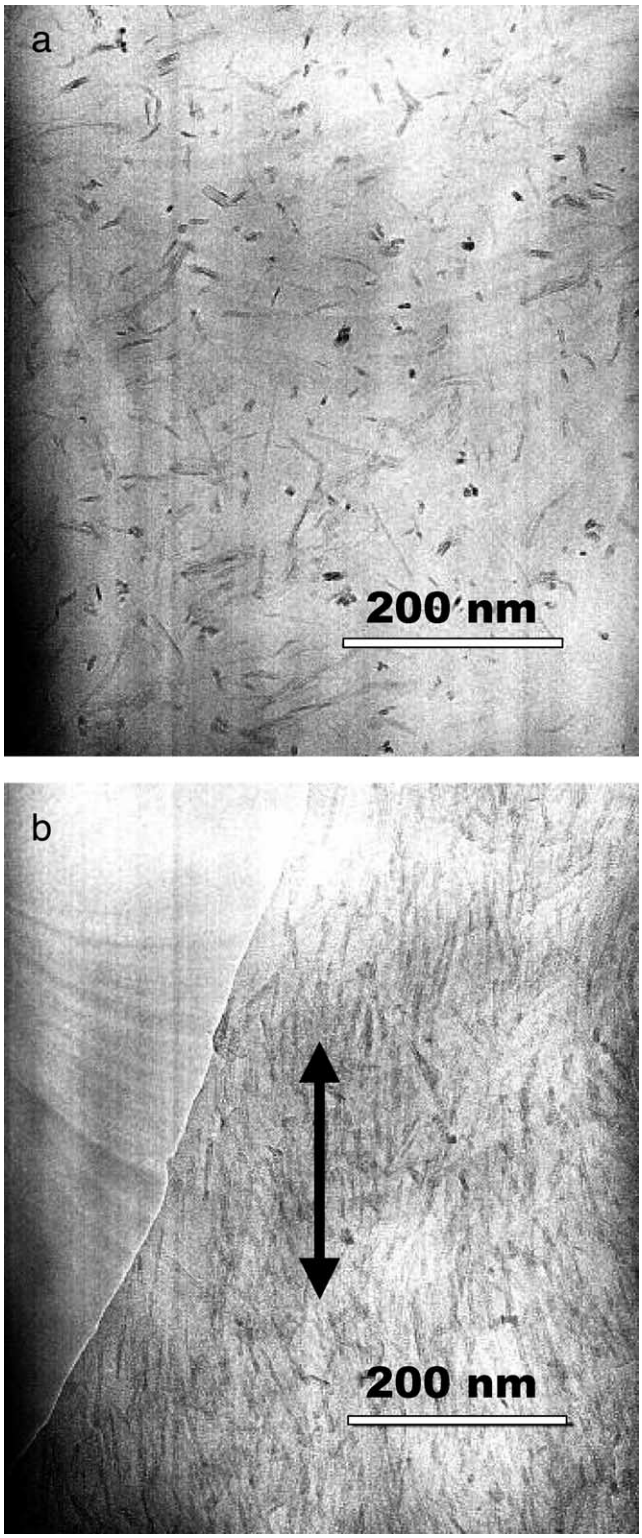

Fig. 1. (a) TEM image of the PA6-BOE7.5 sample. (b) TEM image of the PA6-BOE9 sample.

Fig. 1(b) indicates the preferred direction of the alignment. This observation shows that the high aspect ratio of particles acts as a driving force and leads to the nematic phase formation at 9%. In addition to these, all the samples with boehmite contents lower than 7.5% seem to contain randomly oriented rods as reflected by the optical polarization microscopy results.

3.2. Thermal properties

The DSC curves of the samples were obtained during first heating, cooling and second heating. The first and the second heating curves are of particular interest. The cooling curves are almost identical for all samples and these are not shown. For all of the samples, the crystallization peak appears at 187.5 °C. Fig. 2 shows the first heating curves for PA6's with 9, 7.5, 5, 1.3 and 1% w/w boehmite and that of the neat PA6. The normal melting temperature is around 220 °C for all samples. There is a shoulder around 214 °C, which is very weak for the neat PA6, and becomes more intense with increasing boehmite content. At 7.5%, the intensity of the main peak apparently reduces while the shoulder becomes much more pronounced. Finally, at 9%, the peak at 214 °C dominates over the peak at 221 °C. The first melting at 214 °C is known to be the melting of γ-crystalline phase of PA6 and the high melting peak at 220 °C is due to the α-crystalline structure [14].

Because the first heating results may be influenced by the sample preparation and storage conditions, it is useful to study the second heating to obtain reproducible thermal history of the samples. As the second heating curves in Fig. 3 are concerned, the situation is more complicated and requires careful analysis. For this purpose, curve fitting has been done and rather than using the peak height, the surface areas are compared. Four Gauss functions and a linear baseline were used to fit the DSC curves using the solver in MS-Excel to minimize the sum of squares, by varying the parameters.

In the second heating, the effect of boehmite on the melting peaks is more dramatic. Starting from PA6-BL and throughout the whole concentration range, the γ-peak at about 214 °C, is the major peak. Another difference with respect to the first heating is the emergence of a new peak at about 208 °C. By comparing the melting peaks at various boehmite concentrations, this low temperature peak appears to grow at the expense of the high melting α-peak, so that the chain arrangement is probably similar to the α-structure. As the melting point is reduced one can speculate that this α′-structure forms crystallites with a lower lamellar thickness [15] or involves a distorted lamellar structure arising form the curvature induced by the boehmite cylinders. This should be compared to the observation that in PA6 nanocomposites containing montmorillonite clay platelets a higher melting phase of PA6 has been observed [16]; which probably results from the stabilization of the lamellar crystals. When needles are concerned, one should not necessarily expect the same effect. Because of their geometry, needles should not provide an effective confinement to stabilize the phase, but instead may act as disturbance leading to the formation of less stable crystallites.

As an explanation for the γ-peak being the most intense, it can be argued that after the relatively fast crystallization in the DSC, γ-crystallites may have formed more readily because they require less rearrangement of the polymer chains.

In Table 2, the temperatures and enthalpies for the separate melting processes of α, α′ and γ are given. These are derived from fitted parameters of the second heating curves. Melting temperatures for the α′, γ and α-phases are about the same in all of the samples. In Fig. 4, the $\Delta H_{melt}\alpha'$, $\Delta H_{melt}\gamma$ and $\Delta H_{melt}\alpha$ values from Table 2 are used to obtain a plot against boehmite concentration. In general, ΔH_{melt} of the α-phase decreases with increasing boehmite content, which is an expected trend. Roughly speaking, ΔH_{melt} for

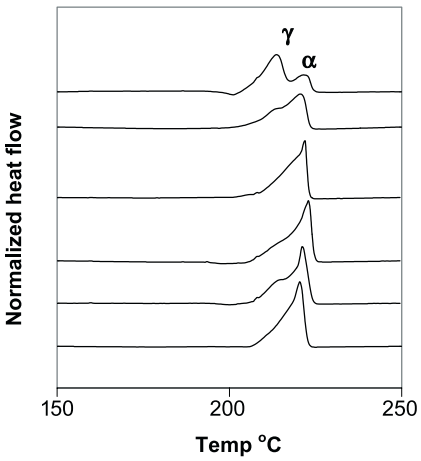

Fig. 2. From top to bottom: DSC first heating curves of PA6 samples containing 9, 7.5, 5, 1.3 and 1% w/w boehmite and the neat PA6 sample.

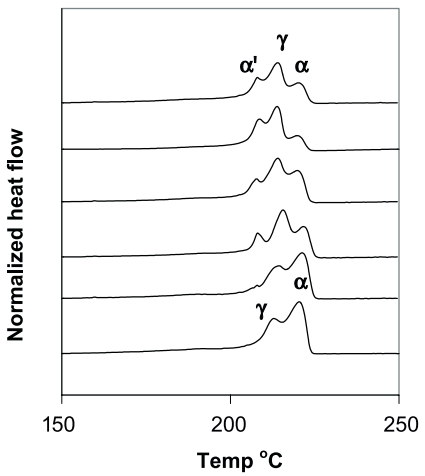

Fig. 3. From top to bottom: DSC second heating curves of PA6 samples containing 9, 7.5, 5, 1.3 and 1% w/w boehmite and the neat PA6 sample.

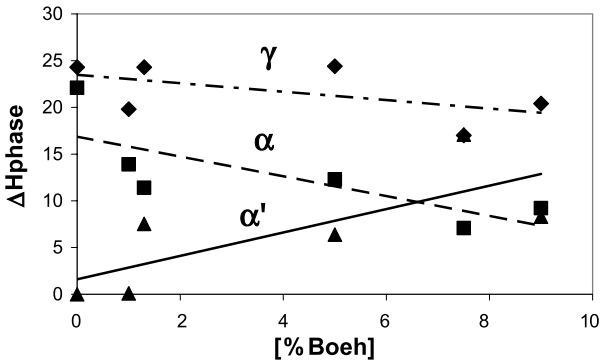

Fig. 4. Enthalpy of melting for the separate phases obtained from the second heating as a function of boehmite concentration.

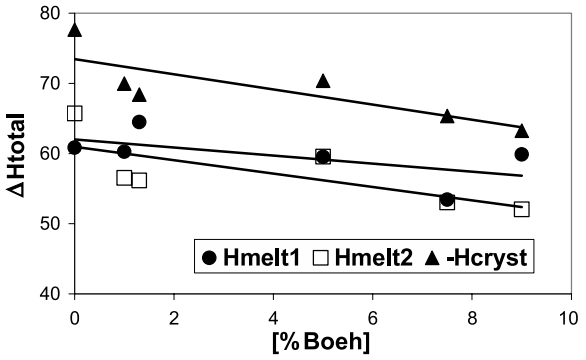

Fig. 5. Total enthalpies of melting and crystallization as a function of boehmite concentration. With $\Delta H_{melt}1$ and 2, the first and the second heating runs are denoted.

the γ-phase is about the same (20–24 J/g) for all of the nanocomposites, regardless of the boehmite content. The only exception is the PA6-BOE7.5 case, where an anomalous drop in the $\Delta H_{melt}\gamma$ is observed. This may be caused by the high degree of confinement of the matrix by the isotropically oriented boehmite particles. The degree of confinement becomes an important issue for PA6-BOE7.5, since it is the isotropic sample with the highest concentration.

The sum of $\Delta H_{melt}\alpha'$ and $\Delta H_{melt}\alpha$ does not change much among the samples which is an indication that these phases are interdependent. There is a clear tendency of α′-phase to form at the expense of α-phase with increasing boehmite content.

In Table 3, total enthalpies of melting and crystallization are given. $\Delta H_{melt}1$ and 2 represent the first and the second heating. In addition, the % crystallinity values for our samples are included in the table. The following relation has been used in calculating the % crystallinity [21]:

$$X_C(\%) = \frac{\Delta H_C}{\Delta H_m^o} 100$$

Here, ΔH_C is the measured enthalpy of crystallization, which is corrected to J/g of PA6. ΔH_m^o is the enthalpy of melting for a 100% crystalline polyamide-6 and is taken as an average value of 190 J/g [21–23].

As seen in Table 3, $\Delta H_{melt}1$ values are close to each other except for PA6-BOE1.3 and PA6-BOE7.5, which have the highest and the lowest $\Delta H_{melt}1$, respectively. We also note that both $\Delta H_{melt}2$ and $-\Delta H_{cryst}$ values show a decreasing trend with increasing boehmite concentration. As % crystallinity values are concerned, these are reasonably close to each other, but decrease slightly at high boehmite contents. For a clear comparison, total enthalpies of melting and crystallization are plotted against boehmite concentration in Fig. 5. Again, the values from Table 3 have been used.

All these observations are in agreement with the behavior reported for PA6 nanocomposites [14–17]. Generally speaking, presence of an inorganic filler results in poor rearrangement of polymer molecules and thus, favors the formation of the γ-phase. In addition, boehmite needles disturb the formation of α-crystallites and induce formation of the less stable α′-phase.

3.3. Mechanical properties

Storage modulus values of the samples have been obtained in the temperature range 37–160 °C. In fact, the measurements have been done in heating from 25 to 160 °C, and then in cooling from 160 to 37 °C. However, the heating part is dedicated to complete removal of moisture from the samples, so only the data from the cooling part will be taken into consideration.

In Fig. 6, the storage moduli vs. temperature plots of the samples are given, within the interval 37–160 °C. In the beginning, with 1% w/w boehmite, there is no mechanical reinforcement. Starting from PA6-BOE1 up to higher concentrations, a systematic increase in the modulus is observed, which is an expected trend. The effect becomes visible at 1.3% w/w boehmite with modulus reaching a

Table 2
Temperatures and enthalpies for the separate melting processes, which occur in the second heating

Sample	$T_{melt}\alpha'$ °C	$\Delta H_{melt}\alpha'$ J/g	$T_{melt}\gamma$ °C	$\Delta H_{melt}\gamma$ J/g	$T_{melt}\alpha$ °C	$\Delta H_{melt}\alpha$ J/g
PA6-BL	–	–	213.4	24.3	220.2	22.1
PA6-BOE1	207.5	0.11	214.2	19.8	221.2	13.9
PA6-BOE1.3	208.2	7.53	215.5	24.3	221.8	11.4
PA6-BOE5	207.4	6.38	214.0	24.4	220.0	12.3
PA6-BOE7.5	208.8	17.1	213.8	17.0	219.6	7.08
PA6-BOE9	207.9	8.30	213.8	20.4	220.2	9.22

Table 3
Total enthalpies of melting (first and second heating) and crystallization and % crystallinity of the samples

Sample	$\Delta H_{melt}1$ J/g	% Crystallinity	ΔH_{cryst} J/g	$\Delta H_{melt}2$ J/g
PA6-BL	60.862	40.9	−77.665	65.714
PA6-BOE1	60.252	36.8	−69.978	56.533
PA6-BOE1.3	64.482	36.0	−68.395	56.159
PA6-BOE5	59.530	37.0	−70.373	59.56
PA6-BOE7.5	53.439	34.4	−65.352	53.036
PA6-BOE9	59.8835	33.3	−63.265	52.044

value of 2.40 GPa. At 5%, the modulus attains a value of 3.73 GPa, which means a 55% increase with respect to the neat sample. Going from 5% to higher concentrations, the theories would expect a further modulus increase, however, this is not observed. First, a sudden decrease from 3.73 to 3.38 GPa is observed at 7.5%, after which it recovers back to 3.74 GPa at 9% boehmite content. It can be argued that for our system, the storage moduli reach a saturation point at some concentration and do not increase any further. This saturation can be the consequence of counteracting effects, which will be discussed in more detail in the next section. Due to the lack of samples with higher boehmite content, it was not possible to determine whether the storage modulus increases any further, or tends to stay constant.

3.4. Mechanical composite models

In order to compare with our real system, several well-known models that generalize the mechanical properties of composites have been employed. First of all, the basic rule of mixtures [18] can be used:

$$E_c = \eta_0 E_f V_f + E_m(1 - V_f)$$

where η_0 is the orientation efficiency factor, which is a function of the angle between the fiber orientation and the applied load.E_f, E_m and E_c are the modulus of the filler, the matrix and the composite, respectively. V_f is the volume fraction of the filler.

In the case of a 2-dimensional isotropic reinforcement, η_0 is taken equal to 3/8. When a 3-dimensional isotropic case is concerned, it is taken as 1/5.

Another widely used model is the one developed by Halpin and Tsai. This model is used for calculating the elastic constants of a unidirectional short fiber composite. Since we are only interested in modulus that is in the longitudinal direction of the short fibers, it is sufficient to calculate the elastic constant only in that direction.

The following are the Halpin–Tsai Eqs. [19]:

$$\frac{M_c}{M_m} = \frac{(1 + \zeta\eta c_r)}{(1 - \eta c_r)}$$

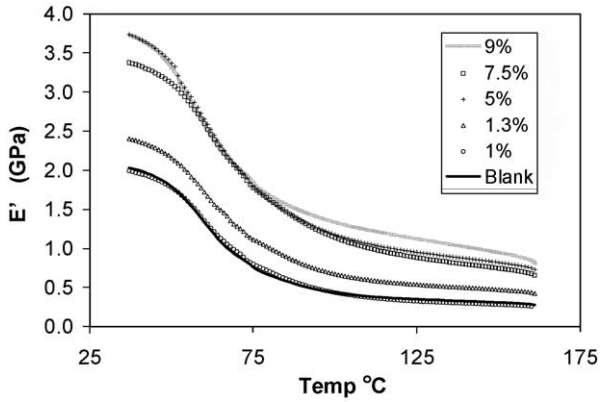

Fig. 6. Storage modulus E' curves of the samples in the temperature interval 37–160 °C, measured at 1 Hz.

where

$$\eta = \frac{\left(\frac{M_r}{M_m} - 1\right)}{\left(\frac{M_r}{M_m} + \zeta\right)}$$

Here, M_c is the modulus of the composite, M_m, of the matrix, M_r is the modulus of the filler, c_r is the volume fraction of the filler, and ζ is a factor that depends on the shape of the filler particle and on the type of modulus to be calculated. To calculate E_{33}—the elastic constant in the longitudinal direction—$\zeta = 2l/d$ is used; where l is the fiber length and d is the fiber thickness.

The equations mentioned above are used to calculate the storage modulus values of our PA6-nanocomposites with varying boehmite concentration. These, together with our experimental values are plotted against boehmite volume fraction as seen in Fig. 7.

For modulus of the matrix, the measured value of 2.03 GPa in the case of neat PA6 has been used. The modulus of the filler has been taken as 253 GPa [20]. In order to convert w/w concentrations into volume fractions, $d_{PA6} = 1.13$ g/cm^3 and $d_{boehmite} = 3.01$ g/cm^3 [4] have been

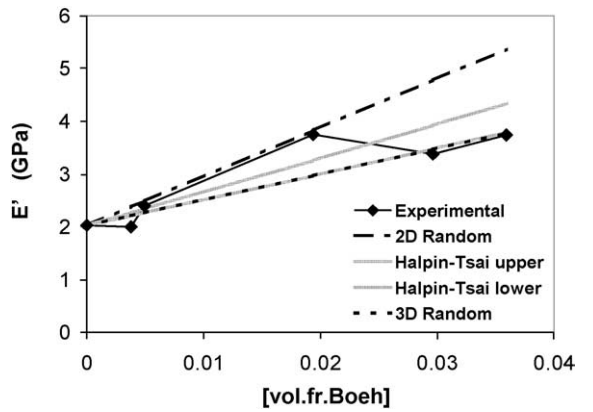

Fig. 7. Comparison of the experimental modulus curve measured at 37 °C, 1 Hz with various composite models as a function of boehmite concentration.

used. For modulus of the nanocomposites, the measured quantities at 37 °C have been substituted.

The experimental curve does not strictly follow any of the theoretical curves, but stays within an acceptable range indicated by these. There exist two Halpin–Tsai curves denoted as upper and lower, which differ only in the ζ factor. In the upper-limit, l/d is taken as 20 and in the lower-limit it is taken as 14. This is because when boehmite is synthesized according to the described method with the given amounts of reactants, the average aspect ratio of particles can vary between 14 and 20. Also, the calculated values for the Halpin–Tsai lower case are very close to the values calculated for the case of 3D-random reinforcement; so that the linear plots seem to coincide.

If the experimental curve is analyzed at volume fractions 0.0076 and 0.019 (1.3% and 5% w/w) the extent of reinforcement is high and this part of the curve follows the 2D-random reinforcement model. At volume fractions 0.028 and 0.062 (7.5% and 9% w/w), the related part of the curve resembles either 3D-random plot or Halpin–Tsai lower plot because they are coincident. This may be explained as a sudden change in the behavior of the system where the poor arrangement of the polymer chains counter-balances the predicted modulus increase at these higher concentrations. Indeed in Table 2, when PA6-BOE7.5 and PA6-BOE9 are concerned, there is a dramatic decrease in $\Delta H_{melt}\alpha$ values and a significant increase in $\Delta H_{melt}\alpha'$ values in comparison to the former sample, PA6-BOE5. This is a clear indication that at these boehmite concentrations, less organized crystalline phases of PA6 are being formed at the expense of the α-phase, which is mainly the reason that we do not observe further reinforcement in our system. The % crystallinity associated with PA6-BOE7.5 and PA6-BOE9 samples are also lower than the others, which can account for the leveling off in modulus.

4. Conclusions

In this work, homogeneous distribution of boehmite particles in a polymer matrix has been described for the first time. Interestingly, the boehmite particles show an isotropic to nematic transition in the polymer, where the nematic phase is obtained at 9% w/w boehmite concentration. Due to the high L/D ratio of the particles, improvement in the polymer Young's modulus is also observed. The results are in good agreement with the 2D random fiber reinforcement model. This improvement, however, does not persist at high boehmite concentrations, but instead tends to level off. We explain this leveling off in modulus by two competing factors: on one hand, mechanical reinforcement of the polymer and on the other, decreasing crystallinity of the matrix polymer. Presence of the particles has also interesting consequences on the organization of the PA6 matrix polymer: with increasing amount of particles, crystallization of the matrix in the γ-structure is favored over the α- and besides, the formation of a low melting α'-phase, an α-phase with reduced crystallite size, is observed. As PA6 is concerned, preferential crystallization in the γ-structure with increasing filler content is a well-known phenomenon in the literature. In our case, the observation of a low melting α'-phase may be a specific one, which may be related to the rod-like shape of the particles. The nematic organization of particles may also add to the shape effect. In future work, the nematic orientation of boehmite rods in the polymer matrix will be examined in more detail.

Acknowledgements

We acknowledge Prof. H.N.W. Lekkerkerker and his group (Colloid Chemistry Group, Utrecht University) for providing knowledge and the experimental set-up in the boehmite synthesis. Dr. P.J. Kooyman of the National Center for High Resolution Electron Microscopy, TU Delft is acknowledged for performing the electron microscopy investigations. Ben Norder of the Polymer and Materials Engineering, TU Delft is highly acknowledged for the DMA and DSC measurements and for his help in the interpretation of the DSC data. This work forms as part of the research program of the Dutch Polymer Institute. In addition, Krzystof Kazimierczak acknowledges the ERASMUS Exchange Program for the financial support.

References

[1] Lagaly G. Appl Clay Sci 1999;15:1–9.
[2] Glaser HR, Wilkes GL. Polym Bull 1989;22:527.
[3] Suzuki F, Onozato K. J Appl Polym Sci 1990;39:371.
[4] Ahmad Z, Sarwar MI, Krug H, Schmidt H. Die Angew Makromol Chem 1997;248:139.
[5] Buining PA, Philipse AP, Lekkerkerker HNW. Langmuir 1994;10:2106.
[6] Davidson P, Batail P, Gabriel JCP, Livage J, Sanchez C, Bourgaux C. Prog Polym Sci 1997;22:913.
[7] Buining PA. Preparation and Properties of Dispersions of Colloidal Boehmite Rods. Utrecht: PhD Thesis, 1992.
[8] Philipse AP, Nechifor AM, Pathmamanoharan C. Langmuir 1994;10:4451.
[9] Van Bruggen MPB. Langmuir 1998;14:2245.
[10] Buining PA, Veldhuizen YSJ, Pathmamanoharan C, Lekkerkerker HNW. Colloids Surf 1992;64:47.
[11] Buining PA, Pathmamanoharan C, Jansen JBH, Lekkerkerker HNW. J Am Ceram Soc 1991;74:1303.
[12] Van Bruggen MPB, Donker M, Lekkerkerker HNW, Hughes TL. Colloids Surf A 1999;150:115.
[13] Pielichowski J, Puszynski A, Polymer preparation methods, Krakow: Technical University of Krakow; 1978.
[14] Wu T, Liao C. Macromol Chem Phys 2000;201:2820.
[15] Kuchta FD, Lemstra PJ, Keller A, Batenburg LF, Fischer HR. Mater Res Soc Symp Proc 2000;628:CC11.12.1.
[16] Van Es M. Polymer-clay nanocomposites. Delft: PhD Thesis, 2001.
[17] Yasue K, Katahira S, Yoshikawa M, Fujimoto K. In: Pinnavaia TJ, Beall G, editors. Polymer-clay nanocomposites. New York: Wiley; 2000. p. 111.

[18] Callister WD. Materials science and engineering: an introduction, 6th ed. New York: Wiley; 2003. p. 535–44.
[19] Ashton JE, Halpin JC, Petit PH. Primer on composite materials: analysis. Technomic Publishing Co; Stamford, USA 1969. Chapter 5.
[20] Gallas MR, Piermarini GJ. J Am Ceram Soc 1994;77:2917.
[21] Liu X, Wu Q, Berglund LA, Qi Z. Macromol Mater Engng 2002;287: 515.
[22] Schultz JM. Polymer crystallization: the development of crystalline order inthermoplastic polymers. Oxford: New York; 2001. p. 82.
[23] Aharoni SM. *n*-Nylons: their synthesis, structure and properties. Wiley: West Sussex; 1997. p. 318–9.